Title

Fluorescent Analogue of Batimastat Enables Imaging of alpha-Secretase in Living Cells

Journal

ACS CHEMICAL NEUROSCIENCE, 7(1)

ISSN

1948-7193

Authors

Leriche, Geoffray
Chen, Allen C
Kim, Sumin
et al.

Publication Date

2016

DOI

10.1021/acschemneuro.5b00283

Peer reviewed

ACS Chemical Neuroscience

Letter

pubs.acs.org/chemneuro

Fluorescent Analogue of Batimastat Enables Imaging of α-Secretase in Living Cells

Geoffray Leriche,[§,†] Allen C. Chen,[§,‡] Sumin Kim,[‡] Dennis J. Selkoe,[‡] and Jerry Yang*[,†]

[†]Department of Chemistry and Biochemistry, University of California, San Diego, La Jolla, California 92093-0358, United States

[‡]Ann Romney Center for Neurologic Diseases, Brigham and Women's Hospital and Harvard Medical School, Boston, Massachusetts 02115, United States

Supporting Information

ABSTRACT: The ADAM family of metalloproteases cleave a diverse range of transmembrane substrates, resulting in the release of their soluble ectodomains. This process of protein shedding, termed α-secretase processing, is involved in many facets of both normal and disease related cellular function. While the processing of substrates has been well documented, the regulation and trafficking of the ADAMs are less well understood. Tools that allow for the study of ADAMs under their native environment will allow for a better understanding of their regulation and activity. Here we describe the design and evaluation of a novel fluorescent analogue of a well-characterized ADAM inhibitor, Batimastat. This probe exhibited similar activity for inhibiting α-secretase processing in cells as did Batimastat. Importantly, this probe specifically labeled ADAMs fluorescently in both fixed and living cells, enabling the possibility to study the trafficking of α-secretase proteins in a dynamic environment.

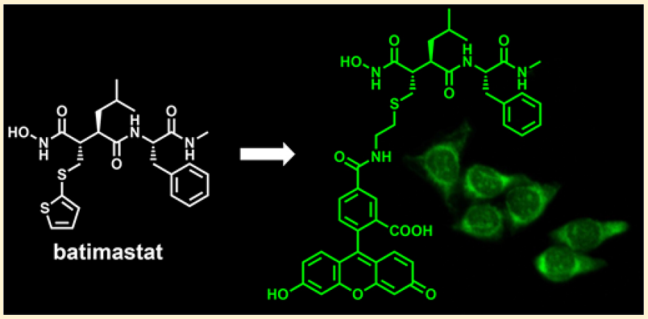

KEYWORDS: *ADAMs, α-secretase, live-cell imaging, probe, fluorescence*

The ADAMs (A Disintegrin And Metalloproteinase) are a family of cell surface transmembrane proteases that function in the shedding of diverse transmembrane proteins including growth factors, cytokines, receptors and adhesion molecules.[1] These cleavage events, termed α-secretase cleavage, play an important role in multiple aspects of basic cell biology.[2] For instance, cleavage of one protein, Notch, is critical for cell differentiation and development, while the processing of another protein, Amyloid Precursor Protein (APP), has implications for Alzheimer's disease (AD) pathology.[3,4] Furthermore, certain mutations found in ADAM10 have been linked to late onset AD.[5,6] There is also emerging evidence for ADAMs as a potential cancer biomarker in cancer diagnosis and predicting patient outcome.[7−9]

The ADAMs are expressed as an immature proenzyme that undergoes a Furin-like cleavage event,[10,11] liberating an inhibitory prodomain and leading to an active protease.[12−14] There are both constitutive and regulated forms of α-secretase activity, which are putatively catalyzed by ADAM10[15] and ADAM17,[16] respectively. The regulation of these proteases is complex and still poorly understood. Chemical probes that target these enzymes could serve as valuable tools to help understand how they are regulated in a dynamic cellular environment.

Small fluorescent probes have been used to reveal the location of proteins within their native environment by fluorescence microscopy. Such fluorescent small-molecule probes that bind specifically to a protein of interest (e.g., kinases,[17] monoamine oxidase A,[18] legumain,[19] cycloxygenase-2,[20] etc.) may offer specific advantages over other methods to track proteins (e.g., fluorescent proteins tags and immunofluorescence). Unlike antibodies, small molecule probes can be readily cell-permeable, which may be useful for dynamically interrogating the intracellular location and movement of proteins in living cells and in vivo. In contrast to tools that exploit the expression of proteins fused to a fluorescent tag (e.g., EGFP), small-molecule probes do not require genetic manipulation of cells that can introduce broad artifacts in protein expression, stability, and localization,[21] and they generally do not alter the structure of the protein, as tags may do.

Here we describe the synthesis and evaluation of a fluorescent analogue of an ADAM inhibitor in order to develop an ADAM-specific, small fluorescent probe for live-cell imaging.

RESULTS AND DISCUSSION

In order to develop a fluorescent probe that could target ADAMs, we based our probe design on the structure of Batimastat (BB94, Figure 1), a potent synthetic inhibitor of ADAMs.[22] BB94 has a low molecular weight and exhibits a peptide-like collagen motif. It comprises a peptide backbone and a hydroxamic acid group, which bind to ADAMs through coordination with the catalytically

Received: October 27, 2015
Accepted: November 11, 2015
Published: November 11, 2015

DOI: 10.1021/acschemneuro.5b00283
ACS Chem. Neurosci. 2016, 7, 40−45

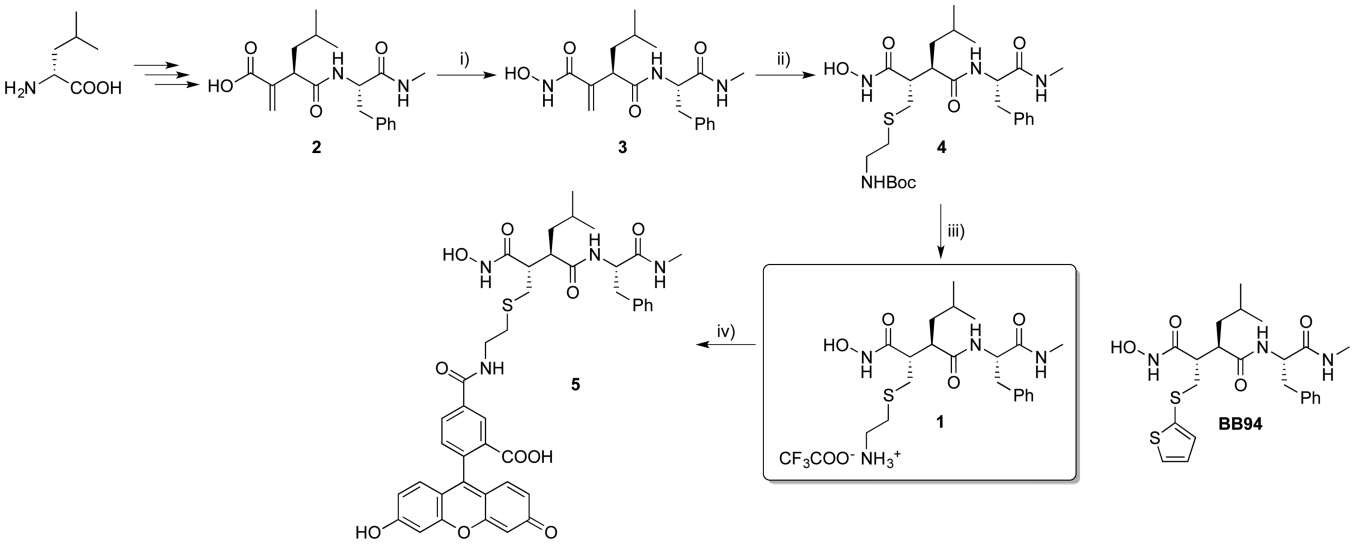

Figure 1. Structures of BB94 and synthetic route for the formation of reactive BB94 analogue **1** and probe **5**. (i) $NH_2OH{\cdot}HCl$, HATU, DBU, TEA, DMF, rt, 16 h (47%); (ii) 2-aminoethanethiol, K_2CO_3, THF, rt, 24 h (45%); (iii) TFA, DCM, 0 °C to rt, 4 h (Qt.); (iv) 5-carboxyfluorescein, PyBOP, TEA, DMF, rt, 16 h (29%).

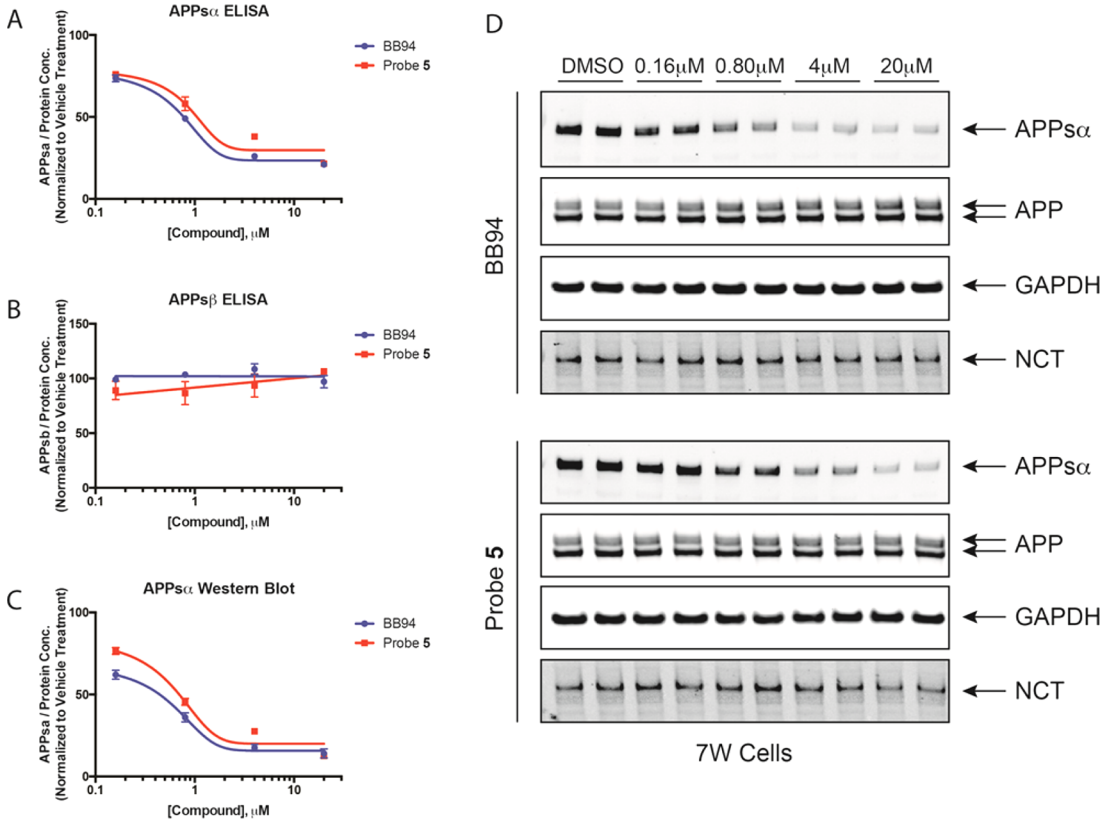

Figure 2. Probe **5** inhibition of α-secretase activity on 7W cells as compared to BB94. (A, B) 7W cells were treated with increasing amounts of either BB94 or Probe **5** (0−20 μM), conditioned media from treated cells were analyzed by an MSD ELISA for APPsα (A) and APPsβ (B). Experiments were performed once in duplicate. (C, D) Conditioned media along with cellular lysates were probed for the protein levels of APPsα, APP, GAPDH, and Nicastrin (NCT) by Western blot (D), and Western blot levels of APPsα were quantified in (C).

active zinc atom.[23] Modified BB94 has been reported previously for the development of an inhibitor-tethered resin for isolation of BB94-targeted proteins from cell lysates.[24] Previous work from structural studies of BB94 bound to a metalloproteinase suggest that the thienyl moiety of BB94 could be replaced with other functionalities without significantly affecting binding to the ADAMs.[25] We, therefore, envisioned that we could replace the thienyl moiety of BB94 with a 2-aminoethanethiol linker, which could later be used for attachment of a fluorophore through reaction of the amine in **1** with an activated carboxylic acid (Figure 1).

Intermediate **2** was initially synthesized from D-leucine using the previously described route (7 steps).[24] Conversion of the carboxylic acid in **2** to the corresponding hydroxamic acid in **3**

DOI: 10.1021/acschemneuro.5b00283
ACS Chem. Neurosci. 2016, 7, 40−45

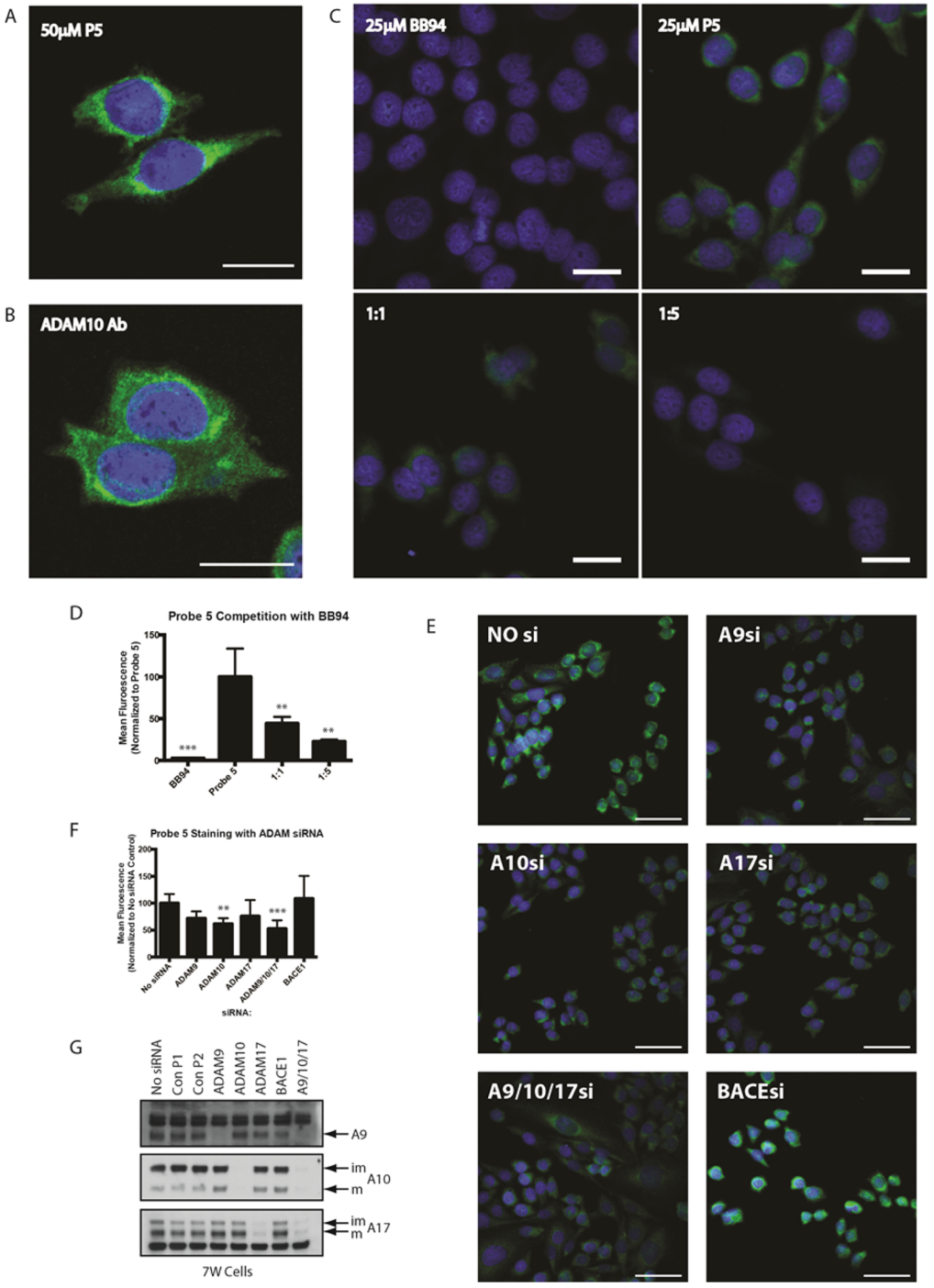

Figure 3. Probe **5** fluorescent staining on 7W cells. (A) Fluorescence imaging on methanol-fixed 7W cells after incubation with 50 μM of probe **5**; scale bar = 20 μm. (B) ADAM10 (PC528, Calbiochem) immunofluorescence on 7W cells; scale bar = 20 μm. (C) Fixed 7W cells were incubated with 25 μM BB94, 25 μM probe **5**, or both simultaneously at a ratio of 1:1 or 1:5; probe **5**/BB94; probe **5** concentration was kept constant at 25 μM; scale bar = 20 μm. (D) Quantitation of (C) using a one-way ANOVA with a Dunnett's post-test comparing all conditions to probe **5** control; $^{**}p < 0.01$, $^{***}p < 0.001$. (E, F) 7W cells were transfected with siRNA targeting ADAM9, 10, 17, 9/10/17, BACE1, or no siRNA as a control, and stained with probe **5** and imaged on a Zeiss LSM-710 (E) and quantitated in (F). A one-way ANOVA using Dunnett's post-test comparing all conditions to No siRNA control was performed; $^{**}p < 0.01$, $^{***}p < 0.001$. (G) Cellular lysates of cells treated with siRNA were probed for the protein levels of ADAM9, ADAM10, and ADAM17 to confirm siRNA engagement of target.

was accomplished using HATU-mediated coupling in the presence of hydroxylamine (Figure 1). The conversion of hydroxamic acid **3** to thioether **4** was carried out with 2-aminoethanethiol in a Michael-type reaction with high stereocontrol as previously reported.[24,26,27] After Boc-deprotection of **3** using trifluoroacetic acid, the resulting amine **1** was engaged in a PYBOP-mediated coupling with 5-carboxyfluorescein (5-FAM) to form fluorescent probe **5** (see Supporting Information, Figure S1). Excitation and emission spectra of probe **5** were recorded and showed retention of the fluorescent properties of the parent fluorophore (see Supporting Information, Figure S2).

DOI: 10.1021/acschemneuro.5b00283
ACS Chem. Neurosci. 2016, 7, 40−45

In order to evaluate the activity of fluorescent BB94 analogue **5**, we initially examined whether this molecule retained the capability to inhibit α-secretase activity in living cells. CHO cells that stably express the canonical α-secretase substrate APP (7W cells)[28] were treated with either probe **5** or BB94 as a control. Conditioned media from treated cells were examined for the levels of APPsα and APPsβ (the products of the α-secretase and β-secretase cleavages of APP, respectively) by a multianalyte ELISA (Figure 2A, B); furthermore, APPsα levels were confirmed by Western blot (Figure 2C, D). Lysates from these cells were also analyzed for the levels of APP, the γ-secretase component Nicastrin (NCT), and GAPDH as a loading control by Western (Figure 2D).

We found that probe **5** exhibited indistinguishable activity for inhibiting the production of APPsα as compared to the parental compound BB94 (Figure 2A, C), with IC50 values of 2.6 and 2.3 μM, respectively. These data suggest that modification of BB94 with a fluorophore as in probe **5** does not appreciably affect the capability of this molecule to engage its target in living cells. As a control, we found no statistically significant effect (P = 0.2191) of probe **5** (0−20 μM) on production of APPsβ in these cellular activity studies (Figure 2B), demonstrating that probe **5** does not have any off-target inhibition of β-secretase. Furthermore, probe **5** did not exhibit general toxicity to 7W cells as compared to BB94, which were both well tolerated by the cells (see Supporting Information, Figure S3).

In order to evaluate the utility of probe **5** for imaging studies, we first stained methanol-fixed 7W cells with a high concentration (50 μM) of probe **5**. Treatment with probe **5** displayed primarily a perinuclear staining pattern (likely endoplasmic reticulum) along with lesser staining throughout the cell body (Figure 3A). This staining pattern was very similar to what was observed when cells underwent fluorescent immunostaining for ADAM10, one of the primary α-secretases[15] (Figure 3B).

In order to evaluate the specificity of probe **5** for BB94-specific targets, we repeated the labeling of cells at a lower concentration (25 μM) of probe **5** in the presence of the nonfluorogenic BB94 compound (Figure 3C). Fluorescence of probe **5** in the cells was reduced to 44% and 23% of the noncompeted probe **5** signal when BB94 was added in a 1:1 or 1:5 ratio of probe **5** to BB94 (Figure 3D). These values are close to the expected theoretical values of 50% and 17% reduction in fluorescence, respectively, if we assume a similar binding affinity of probe **5** and BB94 to ADAM proteins. Therefore, these competition experiments confirm that probe **5** is highly specific for binding to BB94-cellular targets without significant off-target labeling of proteins.

To determine whether probe **5** staining was specific to the ADAMs, we examined the fluorescence staining of probe **5** on 7W cells that were treated with siRNAs targeting three different ADAMs (Figure 3E). siRNA knockdown of ADAM9, 10, 17, or all three ADAMs was able to reduce the staining of probe **5** in cells to 72%, 62%, 76%, and 53% of no siRNA control respectively (Figure 3F). As a control, siRNA knockdown of BACE1, a β-secretase, did not reduce fluorescent labeling by probe **5**, demonstrating that our compound has specificity for α-secretase. Western blot of cellular lysates generated from cells treated with the siRNAs confirmed knockdown of the respective ADAMs (Figure 3G). In these experiments, we knocked down only three of many ADAM proteins that are known to be targeted by BB94.[29] We attribute the remaining fluorescence signal of cells stained with probe **5** after knockdown of ADAM9, 10, and 17 to the labeling of other metalloproteinases (i.e., ADAMs) that are typically targeted by BB94.

To determine whether probe **5** could be used as a tool to label ADAMs in living cells, live 7W cells were incubated with 100 μM of probe **5** in serum-free medium overnight. The following day, cells were imaged by confocal microscopy and the uptake of probe **5** was confirmed by the strong and uniform vesicular pattern of staining of the cells (Figure 4A). We observed a perinuclear staining by probe **5** (Figure 4B) that was similar to that observed in our previous staining of fixed cells (Figure 3A), indicating that probe **5** can be used to stain α-secretase in living cells. As a control, we observed no fluorescence staining in live cells when we used the nonfluorescent parental compound, BB94 (data not shown).

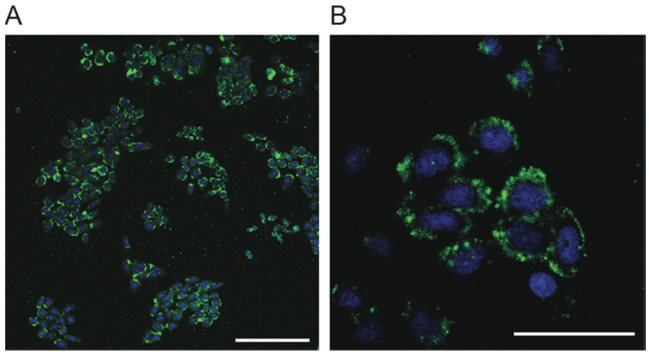

Figure 4. Live cell imaging of probe **5** on 7W Cells. Live 7W cells were treated with 100 μM probe **5** (green channel) and Hoechst (blue channel) and imaged by confocal microscopy at low (A) and high (B) magnifications: Scale bars = 200 and 50 μm for (A) and (B), respectively.

In conclusion, we developed a cell-permeable, fluorophore-conjugated derivative of the α-secretase inhibitor Batimastat (BB94). Once conjugated to a fluorophore, the resulting probe showed no overt cytotoxicity and exhibited activity for inhibiting α-secretase activity that was indistinguishable from the parent compound. Probe **5** also demonstrated a strong selectivity for ADAM staining in both fixed and living cells. These results serve as the foundation for the development of chemical tools to help understand how ADAMs are regulated in a dynamic cellular environment using fluorescence imaging. The application of this probe to study the effects of various protein modulators and phorbol ester treatment on ADAM trafficking and regulation is currently under investigation.

METHODS

Synthesis of probe 5. See the Supporting Information for details.

Cell Culture, Inhibitor Treatments, and siRNA Transfections. 7W CHO cells were grown in standard DMEM plus 10% fetal bovine serum, 2 mM L-glutamine, 100 μg/mL streptomycin, and 100 units/mL of penicillin at 37 °C with 5% CO_2 atmosphere. For inhibitor treatments, BB94 or probe **5** was diluted to the stated concentration in Opti-MEM (Life Technologies) and cells were treated overnight. The following day, conditioned media was collected and cells were harvested in 50 mM HEPES buffer containing 150 mM NaCl and 1% CHAPSO detergent supplemented with protease inhibitor cocktail (Roche). Conditioned media (CM) and lysates were normalized to protein concentration as measured by a BCA assay (Thermo Fisher). For knockdown experiments, siRNA purchased from Dharmacon were transfected with the RNAiMAX reagent (Life Technologies) according to manufacturer's specification. The next day, transfected cells were plated onto a 4-well chamber slide for immunofluorescence and a 6-well plate for biochemistry. At 48 h post transfection, cells in the 4-well chamber slide were fixed and stained, and cells in the 6-well plate were lysed for Western blot.

DOI: 10.1021/acschemneuro.5b00283
ACS Chem. Neurosci. 2016, 7, 40−45

Western Blot and ELISA. CM or cellular lysates were blotted as previously described.[30] Briefly, LDS Sample Buffer (Life Technologies) was added to samples to a final concentration of 1× and heated to 65 °C for 5 min. Samples were then loaded onto a 4−12% Bis-Tris gel (MES buffer) and then transferred to a nitrocellulose membrane. For detection of various proteins, we used AB124695 for ADAM10; AB75609 for ADAM17; a polyclonal antibody from Cell Signaling for ADAM9; a monoclonal antibody from BD Transduction Laboratories for Nicastrin; GAPDH antibody from Millipore; 6E10 or 1736 for APPsα; and an in-house generated antibody C7 for APP. Blots were developed via either ECL or the Odyssey infrared imaging system (LI-COR). For APPs ELISA, we used the multianalyte ELISA kit from Meso Scale Discovery following manufacturer's directions.

Immunofluorescence and Live Cell Imaging. For immunofluorescence of probe **5**, 7W cells were fixed with ice cold methanol for 15 min, followed by blocking with 2% normal donkey serum with 0.1% Triton for 60 min. Probe **5** was diluted in either PBS or ethanol at the specified concentration (with or without competing BB94) and incubated overnight at 4 °C. The next day, cells were washed with 80% ethanol followed by three washes in PBS. DAPI was added to the second PBS wash to stain for the nucleus. Fluorescence was detected by confocal microscopy using a 63× oil immersion objective on a Zeiss LSM-710. For live cell imaging, cells were incubated with 100 μM probe **5** in Opti-MEM media overnight at 37 °C with CO_2. The following day cells were washed with fresh Opti-MEM media, treated with Hoechst for 10 min, washed twice with Opti-MEM, and then imaged with a 10× and 40× air objective.

Quantification and Statistical Analysis. All quantification of Western blots were performed using the Odyssey infrared imaging system (LI-COR), with data normalized to vehicle (DMSO) control. For immunofluorescence images, quantitation was done blinded using ImageJ software, where individual cells were outlined and quantitated. All data were background subtracted and normalized to control. A one-way ANOVA with Dunnett's post-test was performed with significance designated at $p < 0.05$.

■ ASSOCIATED CONTENT

Supporting Information

The Supporting Information is available free of charge on the ACS Publications website at DOI: 10.1021/acschemneuro.5b00283.

Synthetic procedures, UV/vis and fluorescence spectra of probe **5**, ^{1}H NMR spectra, ^{13}C NMR spectra, HPLC traces of probe **5**, and toxicity data (PDF)

■ AUTHOR INFORMATION

Corresponding Author

*E-mail: jerryyang@ucsd.edu. Tel: 858-534-6006. Fax: 858-534-4554.

Author Contributions

§G.L. and A.C.C. contributed equally. G.L., A.C.C., D.J.S., and J.Y. designed the research and analyzed the data; G.L., A.C.C and S.K. executed the experiments, G.L., A.C.C. and J.Y. wrote the manuscript.

Funding

Financial support from the Air Force Office of Scientific Research (FA9550-12-1-0435 (G.L. and J.Y.)) and the National Institutes of Health (AG015379 (D.J.S.)) is gratefully acknowledged. A.C.C. acknowledges support from an NIH T32 institutional training grant (AG000222-19).

Notes

The authors declare no competing financial interest.

■ REFERENCES

(1) Edwards, D. R., Handsley, M. M., and Pennington, C. J. (2008) The ADAM metalloproteinases. *Mol. Aspects Med. 29*, 258−289.

(2) Vingtdeux, V., and Marambaud, P. (2012) Identification and biology of α-secretase. *J. Neurochem. 120*, 34−45.

(3) Postina, R., Schroeder, A., Dewachter, I., Bohl, J., Schmitt, U., Kojro, E., Prinzen, C., Endres, K., Hiemke, C., Blessing, M., Flamez, P., Dequenne, A., Godaux, E., van Leuven, F., and Fahrenholz, F. (2004) A disintegrin-metalloproteinase prevents amyloid plaque formation and hippocampal defects in an Alzheimer disease mouse model. *J. Clin. Invest. 113*, 1456−1464.

(4) Colciaghi, F., Borroni, B., Pastorino, L., Marcello, E., Zimmermann, M., Cattabeni, F., Padovani, A., and Di Luca, M. (2002) [alpha]-Secretase ADAM10 as well as [alpha]APPs is reduced in platelets and CSF of Alzheimer disease patients. *Mol. Med. 8*, 67−74.

(5) Kim, M., Suh, J., Romano, D., Truong, M. H., Mullin, K., Hooli, B., Norton, D., Tesco, G., Elliott, K., Wagner, S. L., Moir, R. D., Becker, K. D., and Tanzi, R. E. (2009) Potential late-onset Alzheimer's disease-associated mutations in the ADAM10 gene attenuate α-secretase activity. *Hum. Mol. Genet. 18*, 3987−3996.

(6) Suh, J., Choi, S. H., Romano, D. M., Gannon, M. A., Lesinski, A. N., Kim, D. Y., and Tanzi, R. E. (2013) ADAM10 missense mutations potentiate β-amyloid accumulation by impairing prodomain chaperone function. *Neuron 80*, 385−401.

(7) Duffy, M. J., Mullooly, M., O'Donovan, N., Sukor, S., Crown, J., Pierce, A., and McGowan, P. M. (2011) The ADAMs family of proteases: new biomarkers and therapeutic targets for cancer? *Clin. proteomics 8*, 9.

(8) Murphy, G. (2008) The ADAMs: signalling scissors in the tumour microenvironment. *Nat. Rev. Cancer 8*, 932−941.

(9) Kessenbrock, K., Plaks, V., and Werb, Z. (2010) Matrix Metalloproteinases: Regulators of the Tumor Microenvironment. *Cell 141*, 52−67.

(10) Hwang, E. M., Kim, S.-K., Sohn, J.-H., Lee, J. Y., Kim, Y., Kim, Y. S., and Mook-Jung, I. (2006) Furin is an endogenous regulator of α-secretase associated APP processing. *Biochem. Biophys. Res. Commun. 349*, 654−659.

(11) Anders, A., Gilbert, S., Garten, W., Postina, R., and Fahrenholz, F. (2001) Regulation of the alpha-secretase ADAM10 by its prodomain and proprotein convertases. *FASEB J. 15*, 1837−1839.

(12) Moss, M. L., Bomar, M., Liu, Q., Sage, H., Dempsey, P., Lenhart, P. M., Gillispie, P. A., Stoeck, A., Wildeboer, D., Bartsch, J. W., Palmisano, R., and Zhou, P. (2007) The ADAM10 Prodomain Is a Specific Inhibitor of ADAM10 Proteolytic Activity and Inhibits Cellular Shedding Events. *J. Biol. Chem. 282*, 35712−35721.

(13) Gonzales, P. E., Solomon, A., Miller, A. B., Leesnitzer, M. A., Sagi, I., and Milla, M. E. (2004) Inhibition of the Tumor Necrosis Factor-α-converting Enzyme by Its Pro Domain. *J. Biol. Chem. 279*, 31638−31645.

(14) Allinson, T. M. J., Parkin, E. T., Turner, A. J., and Hooper, N. M. (2003) ADAMs family members as amyloid precursor protein alpha-secretases. *J. Neurosci. Res. 74*, 342−352.

(15) Kuhn, P.-H., Wang, H., Dislich, B., Colombo, A., Zeitschel, U., Ellwart, J. W., Kremmer, E., Roßner, S., and Lichtenthaler, S. F. (2010) ADAM10 is the physiologically relevant, constitutive α-secretase of the amyloid precursor protein in primary neurons. *EMBO J. 29*, 3020−3032.

(16) Buxbaum, J. D., Liu, K. N., Luo, Y., Slack, J. L., Stocking, K. L., Peschon, J. J., Johnson, R. S., Castner, B. J., Cerretti, D. P., and Black, R. A. (1998) Evidence that tumor necrosis factor alpha converting enzyme is involved in regulated alpha-secretase cleavage of the Alzheimer amyloid protein precursor. *J. Biol. Chem. 273*, 27765−27767.

(17) Zhang, Z., Kwiatkowski, N., Zeng, H., Lim, S. M., Gray, N. S., Zhang, W., and Yang, P. L. (2012) Leveraging kinase inhibitors to develop small molecule tools for imaging kinases by fluorescence microscopy. *Mol. BioSyst. 8*, 2523−2526.

(18) Wu, J. B., Lin, T.-P., Gallagher, J. D., Kushal, S., Chung, L. W. K., Zhau, H. E., Olenyuk, B. Z., and Shih, J. C. (2015) Monoamine oxidase A inhibitor-near-infrared dye conjugate reduces prostate tumor growth. *J. Am. Chem. Soc. 137*, 2366−2374.

(19) Lee, J., and Bogyo, M. (2010) Development of near-infrared fluorophore (NIRF)-labeled activity-based probes for in vivo imaging of legumain. *ACS Chem. Biol. 5*, 233−243.

DOI: 10.1021/acschemneuro.5b00283
ACS Chem. Neurosci. 2016, 7, 40−45

(20) Uddin, M. J., Crews, B. C., Ghebreselasie, K., and Marnett, L. J. (2013) Design, synthesis, and structure-activity relationship studies of fluorescent inhibitors of cycloxygenase-2 as targeted optical imaging agents. *Bioconjugate Chem. 24*, 712−273.
(21) Kobayashi, H., Ogawa, M., Alford, R., Choyke, P. L., and Urano, Y. (2010) New strategies for fluorescent probe design in medical diagnostic imaging. *Chem. Rev. 110*, 2620−2640.
(22) Brown, P. D., and Giavazzi, R. (1995) Matrix metalloproteinase inhibition: A review of anti- tumour activity. *Ann. Oncol. 6*, 967−974.
(23) Grams, F., Crimmin, M., Hinnes, L., Huxley, P., Pieper, M., Tschesche, H., and Bode, W. (1995) Structure determination and analysis of human neutrophil collagenase complexed with a hydroxamate inhibitor. *Biochemistry 34*, 14012−14020.
(24) Hesek, D., Toth, M., Krchnak, V., Fridman, R., and Mobashery, S. (2006) Synthesis of an inhibitor-tethered resin for detection of active matrix metalloproteinases involved in disease. *J. Org. Chem. 71*, 5848−5854.
(25) Lang, R., Kocourek, A., Braun, M., Tschesche, H., Huber, R., Bode, W., and Maskos, K. (2001) Substrate specificity determinants of human macrophage elastase (MMP-12) based on the 1.1 Å crystal structure. *J. Mol. Biol. 312*, 731−742.
(26) Hirayama, R., Yamamoto, M., Tsukida, T., Matsuo, K., Obata, Y., Sakamoto, F., and Ikeda, S. (1997) Synthesis and biological evaluation of orally active matrix metalloproteinase inhibitors. *Bioorg. Med. Chem. 5*, 765−778.
(27) Bailey, S., Bolognese, B., Buckle, D. R., Faller, A., Jackson, S., Louis-Flamberg, P., McCord, M., Mayer, R. J., Marshall, L. A., and Smith, D. G. (1998) Selective inhibition of low affinity IgE receptor (CD23) processing. *Bioorg. Med. Chem. Lett. 8*, 29−34.
(28) Koo, E. H., and Squazzo, S. L. (1994) Evidence that production and release of amyloid beta-protein involves the endocytic pathway. *J. Biol. Chem. 269*, 17386−17389.
(29) Reiss, K., and Saftig, P. (2009) The "a disintegrin and metalloprotease" (ADAM) family of sheddases: Physiological and cellular functions. *Semin. Cell Dev. Biol. 20*, 126−137.
(30) Chen, A. C., Guo, L. Y., Ostaszewski, B. L., Selkoe, D. J., and LaVoie, M. J. (2010) Aph-1 Associates Directly with Full-length and C-terminal Fragments of -Secretase Substrates. *J. Biol. Chem. 285*, 11378−11391.

DOI: 10.1021/acschemneuro.5b00283
ACS Chem. Neurosci. 2016, 7, 40−45